Science World Journal Vol. 16(No 3) 2021
www.scienceworldjournal.org
ISSN: 1597-6343 (Online), ISSN: 2756-391X (Print)
Published by Faculty of Science, Kaduna State University

Full Length Research Article

ANALYSIS AND INTERPRETATION OF HIGH RESOLUTION AEROMAGNETIC DATA OF ABUJA SHEET 186 AND GITATA SHEET 187, CENTRAL NIGERIA

[1]Oguche, Monday*, [1]Akanbi, Eti-mbuk Stella and [2]Odewumi, Shola Christopher

[1]Department of Physics, University of Jos, Nigeria.
[2]Department of Science Laboratory Technology, University of Jos, Nigeria.

*Corresponding Author Email Address: senatoroguche@gmail.com

ABSTRACT
Analysis of high resolution aeromagnetic data of Abuja Sheet 186 and Gitata Sheet 187, North Central Nigeria were carried out. The geomagnetic gradient was removed from the aeromagnetic data using the International Geomagnetic Reference Field (IGRF) and the obtained result was shown as Total Magnetic Intensity (TMI) maps. Software used for the analysis include: Oasis Montaj Version 8.4, Matlab Version R2010a, Grapher 5, SUFER 11, Georient and Microsoft Excel. The regional magnetic values range from 33213.0 to 33361.4 nT. The SW region is associated with lower magnetic values ranging from 33213.0 to 33222.0nT while the NE portion of the map is marked with higher aeromagnetic values ranging from 33352.3 to 33361.4nT. The residual field values range from -392.5 to -171.6 nT and the negative residuals dominate the study area because the study area is dominated by sediments and located at the western part of the magnetic equator. The reduced-to-equator map shows similar features with the crustal field map except for re-alignment of anomalies. The magnetic intensity ranges from -177.1 to -388.9 nT and first vertical derivative ranges from -0.190 to 0.161 nT/km. The fractures largely trend in the NE-SW and NW-SE directions. The Source Parameter Imaging revealed depth ranging from 45.0 to 378.3 m and the dominant geological features are sills and dykes. The depth (D2) to the shallow magnetic sources varies from 0.253 to 0.728 km while the depth (D1) to the magnetic basement varies from 0.479 to 3.36 km.

Keywords: Shallow, Deeper, Magnetic residual, Lineaments, Abuja and Gitata.

INTRODUCTION

The magnetism of the interior part of the earth is made up of three parts: Core, Mantle and Crust. Our planet's magnetic field is believed to be generated deep down in the Earth's core (Reynolds, 2005). The interaction of such fields with the Earth's primary field gives rise to the field at the Earth's surface (Reeves, 2005).

The measured magnetic field is the resultant of the Earth's magnetic field and the anomaly field. The shape and amplitude of a magnetic anomaly depends on the location, shape, size, strike, burial depth, magnetic susceptibility, and intrinsic magnetisation of the causative body, and the angle at which the survey lies relative to both the Earth's magnetic field and to the causative body. (Reynolds, 1990).

Magnetization of rocks is extremely variable depending on the type of rocks and environment the rock is located. These anomalies in the earth's magnetic field are caused by remnant and induced magnetism (Reeves, 2005). The aim of this study is to analyse and interpret the high resolution aeromagnetic data acquired in 2009 covering Abuja sheet and Gitata, North-central Nigeria.

Location and Geology of Study Area

The study area covers longitudes 7˚ 00' to 8˚ 00'E and latitudes 9˚ 00' to 9˚30'N (Figure 1) with estimated area of 6,050km^2. The topography is rugged and undulating with the Basement rocks outcropping as hills and inselbergs. The Gwagwa plains occurring at the west of the Federal Capital Territory (FCT) are underlain by migmatites and gneisses (Figure 1 & 2). These plains form part of River Abuja that originates in the Bwari-Aso hills, north-eastern part of Abuja (Figure 1). The drainage pattern varies from trellis to dendritic and is drained by Rivers Gwagwalada and Abuja (Figure 1).

The study area is almost predominantly underlain by high-grade metamorphic and igneous rocks of Precambrian age generally trending NW – SE (Obaje, 2009). These rocks consists of Medium-grained Biotite granite, Biotite Hornblende granite, Granite Gneiss, Quartzite, Undifferentiated Older Granite, Porphryroblastic Gneiss, Coarse Porphyritic Biotite hornblende Granite, Migmatite Gneiss and migmatites as shown in figure 2.

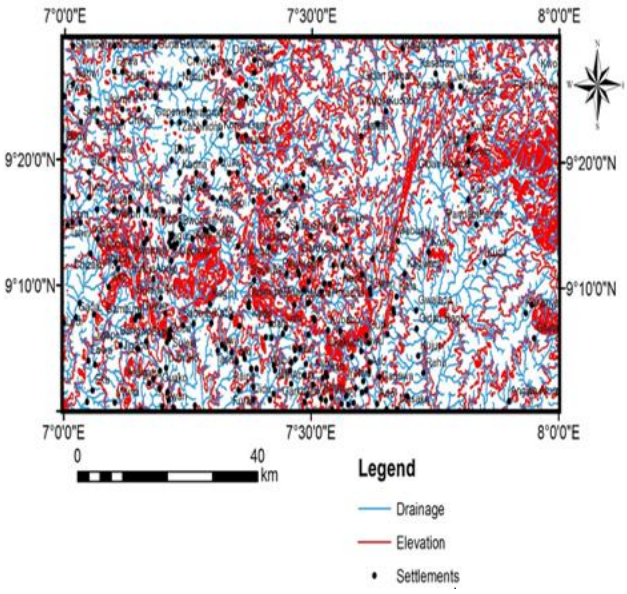

Figure 1: Topographical Map of the Study Area (Extracted from Topographical map of Abuja Sheet 186 and Gitata Sheet 187, Nigerian Geological Survey, 1962)

Science World Journal Vol. 16(No 3) 2021
www.scienceworldjournal.org
ISSN: 1597-6343 (Online), ISSN: 2756-391X (Print)
Published by Faculty of Science, Kaduna State University

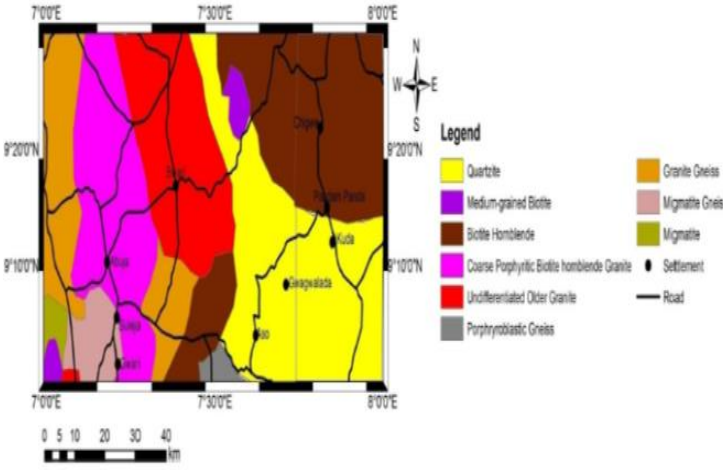

Figure 2: Geological Map of the Study area (Extracted from Geology map of Abuja Sheet 186 and Gitata Sheet 187, Nigerian Geological Survey Agency, 1963)

MATERIALS AND METHODS

The aeromagnetic maps used for the study were acquired from the Nigeria Geological Survey Agency (2009). This data is high resolution aeromagnetic map. The nominal flight height of 80 m along N-S flight lines spaced at 500 m interval using advanced equipment with far higher resolution was used. The geomagnetic gradient was removed from the data using the International Geomagnetic Reference Field (IGRF) and the obtained data are shown as Total Magnetic Intensity (TMI) maps. Software used for the analysis are: Oasis Montaj Version 8.4, Matlab Version R2010a, Grapher 5, SUFER 11, Georient and Microsoft Excel.

The Total Magnetic Intensity data were subjected to regional residual separation filter to obtain the residual data (crustal field). The RTE was applied to the Crustal (residual) map and the crustal field map was used to obtain the Reduced –to- Equator map. Using the Geosoft extensions on the Load or GX menu, On the MAGMAP menu, MAGMAP 1- step filtering was selected to automatically open the dialogue box (Magmap Filter Design). On the dialog box the filter option was selected to obtain the template to reduce-to-equator. Survey date was inputted and the calculated button was employed to automatically calculate the required fields for the reduction to equator.

The First Vertical Derivative using RTE was processed with respect to x, y and z, with their derivatives dx, dy and dz respectively. The FVD data was used to obtain the lineament arch as well as the rose diagram plot (figure 10). The ticks drawn out (i.e. lineaments) are now used to plot the Rose diagram using ArcGIS. The result of the lineaments was stored in a tabular format. The purpose of upward continuation is vital in discovering geological anomalies. In this numerical technique the Reduced-to-Equator data was projected at an elevation to a higher elevation. The principle is not far-fetched from the fact that short-wavelength features are attenuated or smoothed out while long-wavelength features are enhanced.

The Source Parameter Imaging TM (SPITM) function is a quick, easy, and powerful method for calculating the depth of magnetic sources. Its accuracy has been shown to be +/- 20% in tests on real data sets with drill-hole control. This accuracy is similar to that of Euler deconvolution, however SPI has the advantage of producing a more complete set of coherent solution points and it is easier to use. The SPI method (Thurston and Smith, 1997) estimates the depth from the local wave number of the analytical signal. The analytical signal $A_1(x, z)$ is defined by Nabighian (1972) as:

$$A_1(x,z) = \frac{\partial \mathrm{M}(x,z)}{\partial \mathrm{x}} - j\frac{\partial \mathrm{M}(x,z)}{\partial \mathrm{z}} \quad (1)$$

where M (x, z) is the magnitude of the anomalous total magnetic field, j is the imaginary number, z and x are Cartesian coordinates for the vertical direction and the horizontal direction respectively. The horizontal and vertical derivatives comprising the real and imaginary parts of the 2D analytical signal are related as follows:

$$\frac{\partial \mathrm{M}(x,z)}{\partial \mathrm{x}} \Leftrightarrow -\frac{\partial \mathrm{M}(x,z)}{\partial \mathrm{z}} \quad (2)$$

Where⇔denotes a Hilbert transformation pair. The local wave number k_1 is defined by Thurston and Smith (1997) to be:

$$k_1 = \frac{\partial}{\partial x}\tan^{-1}\left\langle \frac{\partial M}{\partial z} \middle| \frac{\partial M}{\partial x} \right\rangle \quad (3)$$

The concept of an analytic signal comprising second-order derivatives of the total field, if used in a manner similar to that used by the Hilbert transform and the vertical-derivative of equation 2 will give the Hilbert transform pair.

$$\frac{\partial^2 \mathrm{M}(x,z)}{\partial z \partial \mathrm{x}} \Leftrightarrow -\frac{\partial^2 \mathrm{M}(x,z)}{\partial^2 \mathrm{z}} \quad (4)$$

Thus, the analytic signal could be defined based on second-order derivatives, $A_2(x, z)$ is given as (Nabighian (1972)

$$A_2(x,z) = \frac{\partial^2 \mathrm{M}(x,z)}{\partial z \partial \mathrm{x}} - j\frac{\partial^2 \mathrm{M}(x,z)}{\partial^2 \mathrm{z}} \quad (5)$$

The second-order local wave number *k_2 is given as*

$$k_2 = \frac{\partial}{\partial x}\tan^{-1}\left\langle \frac{\partial^2 M}{\partial^2 z} \middle| \frac{\partial^2 M}{\partial z \partial x} \right\rangle \quad (6)$$

RESULTS

The Total Magnetic Intensity map shows value ranging from 32919.5to 33083.5nT (Figure 3). The regional magnetic values ranging from 33213.0 to 33361.4 nT (Figure 4) while Figure 5 shows the residual magnetic values ranging from -392.5 to -171.6 nT. The reduced-to-equator (RTE) map shows magnetic intensity value ranging from -388.9 to -177.1 nT (Figure 6). The upward continued RTE field to 3km ranges from -185 to 186 nT/km (Figure 7). This is greater than the field obtained from the upward continued RTE field to15km of -351.0 to -194.3 nT/km (Figure 8). The First Vertical Derivative (FVD) map has an intensity ranging from -0.190 to 0.161 nT/km (Figure 9) and lineaments extracted from the FVD map are shown in Figure 10.

The locations of grids and the computed spectral depths are presented in Table 1 with X_1 and X_2as the limiting longitudes while $Y_1$and Y_2as the limiting latitudes for each of the blocks. Each of these plots revealed a two-layer depth model as represented by two clear segments. Thus, the logarithmic plot of a radial spectrum would give a straight line whose slope is 2z. From the gradients of the segments, the average depths to the causative layers were determined as D_1 and D_2. The first layer depth (D_2) represents the depth to the shallow magnetic sources while the depth (D_1) to the magnetic basement (sedimentary thickness) is represented by the

Science World Journal Vol. 16(No 3) 2021
www.scienceworldjournal.org
ISSN: 1597-6343 (Online), ISSN: 2756-391X (Print)
Published by Faculty of Science, Kaduna State University

second line segment of the power spectrum plots.

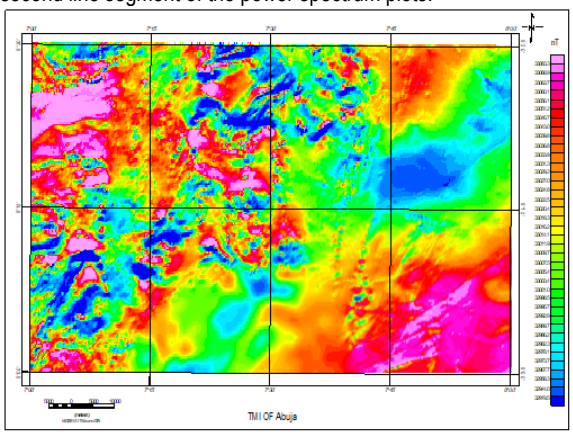

Figure 3: Total Magnetic Intensity Map of Abuja Sheet 186 and Gitata Sheet 187 (Source: NGSA, 2009)

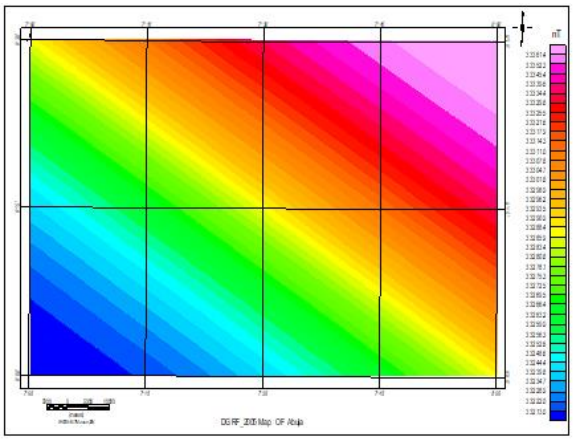

Figure 4: Regional Field Map of the Abuja sheet 186 and Gitata sheet 187

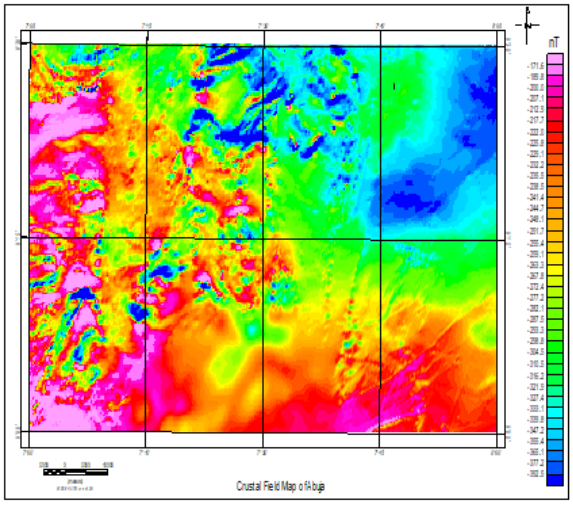

Figure 5. Residual or Crustal Field Map of Abuja sheet 186 and Gitata Sheet 187

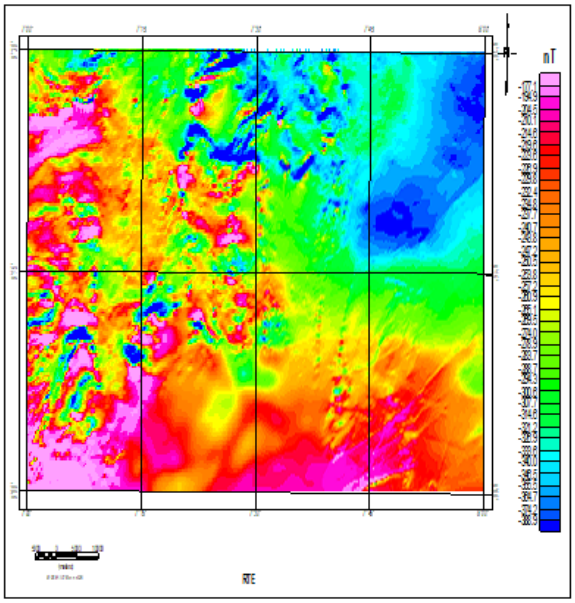

Figure 6: Reduced to equator map of Abuja sheet 186 and Gitata sheet 187

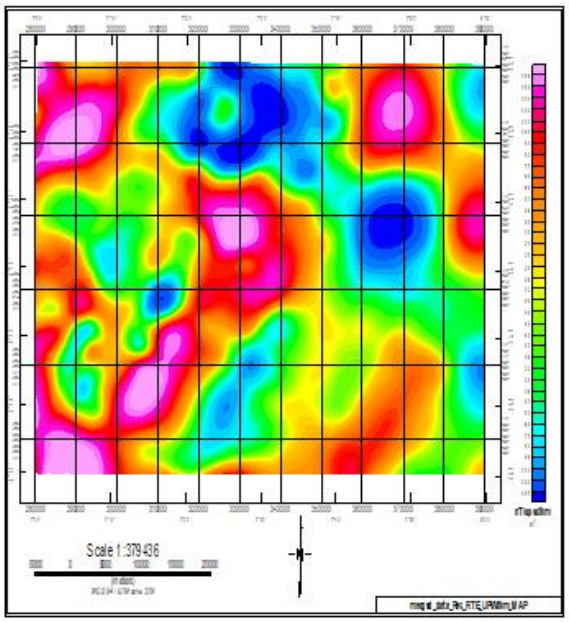

Figure 7: Upward Continuation Map of Abuja sheet 186 and Gitata Sheet 187 to 3km

Science World Journal Vol. 16(No 3) 2021
www.scienceworldjournal.org
ISSN: 1597-6343 (Online), ISSN: 2756-391X (Print)
Published by Faculty of Science, Kaduna State University

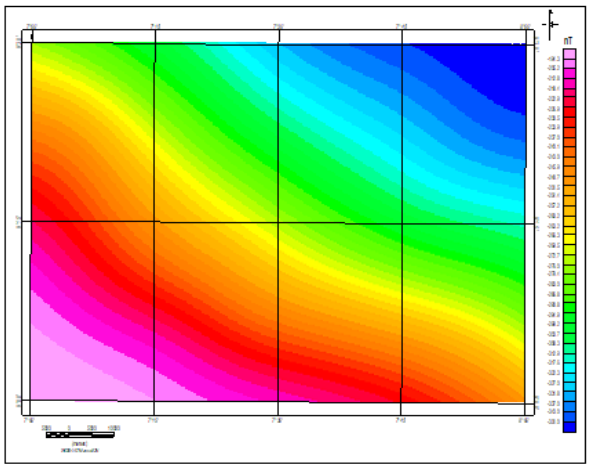

Figure 8: Upward Continuation Map of Abuja sheet 186 and Gitata Sheet 187 to 15km

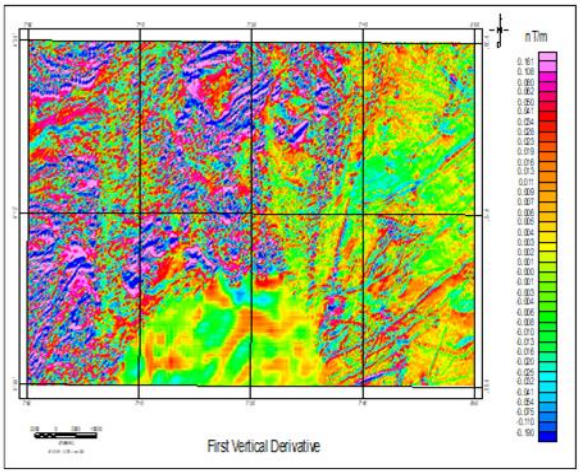

Figure 9: First Vertical Derivatives (FVD) map of Abuja sheet 186 and Gitata sheet 187

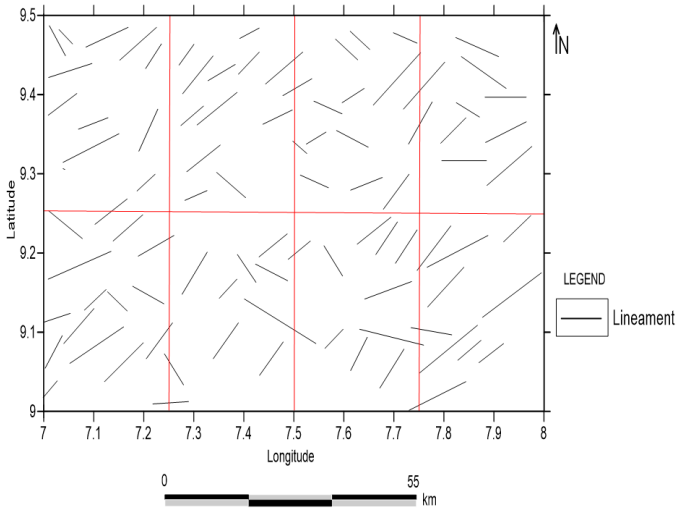

Figure 10: Lineament Archs Extracted from FVD of Abuja sheet 186 and Gitata Sheet 187

Table 1: Spectral Depth Estimates to Magnetic Basement over Abuja sheet 186 and Gitata sheet 187 [D_1=Deeper Source (km) and D_2= Shallow source (km)].

Spectral Block	Longitude (°)		Latitude (°)		Spectral Depth (km)	
	X_1	X_2	Y_1	Y_2	D_1	D_2
1	7.000	7.125	9.375	9.500	1.760	0.368
2	7.125	7.250	9.375	9.500	1.840	0.467
3	7.250	7.375	9.375	9.500	0.521	0.327
4	7.375	7.500	9.375	9.500	1.300	0.327
5	7.500	7.625	9.375	9.500	0.719	0.303
6	7.625	7.750	9.375	9.500	0.654	0.333
7	7.750	7.875	9.375	9.500	3.360	0.578
8	7.875	8.000	9.375	9.500	1.320	0.345
9	7.000	7.125	9.250	9.375	0.650	0.351
10	7.125	7.250	9.250	9.375	0.645	0.292
11	7.250	7.375	9.250	9.375	0.642	0.333
12	7.375	7.500	9.250	9.375	2.520	0.547
13	7.500	7.625	9.250	9.375	0.611	0.253
14	7.625	7.750	9.250	9.375	0.790	0.308
15	7.750	7.875	9.250	9.375	2.720	0.482
16	7.875	8.000	9.250	9.375	1.280	0.403
17	7.000	7.125	9.125	9.250	0.624	0.335
18	7.125	7.250	9.125	9.250	0.539	0.354
19	7.250	7.375	9.125	9.250	0.530	0.379
20	7.375	7.500	9.125	9.250	2.860	0.443
21	7.500	7.625	9.125	9.250	1.170	0.328
22	7.625	7.750	9.125	9.250	2.580	0.728
23	7.750	7.875	9.125	9.250	0.942	0.317
24	7.875	8.000	9.125	9.250	1.210	0.472
25	7.000	7.125	9.000	9.125	0.483	0.289
26	7.125	7.250	9.000	9.125	0.734	0.364
27	7.250	7.375	9.000	9.125	1.730	0.465
28	7.375	7.500	9.000	9.125	1.120	0.411
29	7.500	7.625	9.000	9.125	1.480	0.445
30	7.625	7.750	9.000	9.125	0.479	0.353
31	7.750	7.875	9.000	9.125	2.100	0.337
32	7.875	8.000	9.000	9.125	0.887	0.300
	Average spectral depth				1.275	0.386

DISCUSSION

The total magnetic intensity map (Figure 3) shows the variation in either lithology or basement topography. The total magnetic intensity map (Figure 3) indicates the variation in magnetic intensity and ranges from 32919.5 to 33083.5nT. The high TMI value as shown in Figure 3 located at the southern part of Gitata sheet depicts the presence of quartzite and granite-gneiss around Gwagwalada-Kuda areas (Figure 2) while the low TMI value indicates biotite-hornblende granite around Chigwe (Figure 2). The magnetic intensity values obtained in this research (32919.5-33083.5nT) is similar with TMI values of 33161.8 to 33471.8nT reported by Adewumi and Salako (2017) and TMI values of 32750 to 32900nT reported by Ajakaiye et al. (1985) in north central Nigeria. This means that the regional magnetic values due to the core and crustal or residual values due to magnetic signatures between this research work and the research reported by both Adewumi-Salako and Ajakaiye share common similarities on the values recorded.

Science World Journal Vol. 16(No 3) 2021
www.scienceworldjournal.org
ISSN: 1597-6343 (Online), ISSN: 2756-391X (Print)
Published by Faculty of Science, Kaduna State University

The regional magnetic values range from 33213.0 to 33361.4 nT with a trending pattern along SE-NW directions (Figure 4). The SW region is associated with lower magnetic values ranging from 33213.0 to 33222.0nT while the NE portion of the map is marked with higher aeromagnetic values ranging from 33352.3 to 33361.4nT. These are the crustal field, residual anomalies, residual field or simply residuals which may provide evidence of the existence of mineral ore bodies or reservoir-type structures.

The residual field values range from -392.5 to -171.6 nT (Figure 5). Negative residuals dominate the study area because the study area is close to the magnetic equator. Low residual values were observed in north-eastern part of Abuja and Gitata sheets with an intensity value of -392.5 to -287.5nT and Quiet area was observed with an intensity value of -304.5 to -251.7nT. The anomalies observed are in form of closures, which could be as a result of circular features, long narrow anomaly and dislocation, mostly around NW and SW of the study area (Figure 5). The circular patterns are usually associated with granite intrusion or ore bodies while narrow patterns are frequently due to dykes, tectonic shear zones and long ore bodies(Parasnis, 1997).The nature of the closure depicts the depth of burial and size of intrusions that are within the basement underlying the area (Parasnis, 1997). Short to moderately long dislocations were also noticed in the magnetic map, which is indicative of short to moderately long geologic faults.

The reduced-to-equator map shows magnetic intensity ranging from -177.1 to -388.9 nT (Figure 6) with high intensity anomalies and very few locations identified with low intensity anomalies. The anomalies are mostly trending in the NE-SW and NW-SE directions. The regions with highest magnetic intensity of -171.6to -189.8 nT could be underlain by migmatite and associated with high magnetic values observed due to iron rich content of the rock unit.

The magnetic intensity of 3km ranges from -185 to 186 nT/km (Figure 7) which is greater than the intensity of 15km map which ranges from -351.0 to -194.3 nT/km (Figure 8). In the 3km map, the negative intensity anomaly (blue) ranges from -185 to 186 nT/km and appears as a large rounded anomaly trending in the NE-SW direction underlain by quartzite and biotite hornblende granite. Similarly, the positive intensity anomaly (violet) appears at the NW, NE, North central and SW of the map underlain by migmatite gneiss, granite gneiss and biotite hornblende. At 15km, upward continued trends SE-NW and the highest value of the upward continued intensity occurs in the south-western part while the lowest value of the upward continued intensity occurs in the northeaster part (Figure 8).

The major reason for upward continuing to 15km is to determine the curie depth, Curie temperature, geothermal gradient and heat flow. At this depth of 15km the rock must have lost its magnetization properties (Bello, 2017). The report of Ganiyu et al. (2012) on Aeromagnetic Data of Ibadan area shows similar change in anomaly character with increasing observation to magnetic source distance as RTE was upward continued to 15km. The report of Akanbi and Fakoya (2015) was upward continued at 1km, 2km and 3km in Maijuju area while this study wasupward continued at 3km and 15 km. The findings of Akanbi and Fakoya (2015) displayed similarity in terms of short wave length for shallow magnetic sources and long wave length for deep seated magnetic sources as observed in this study.

The FVD has an intensity ranging from -0.190 to 0.161 nT/km and the anomaly largely trend in the NE-SW and NW-SE directions (Figure 9). These trends compare qualitatively with the orientational analysis of lineament arch (Figure 10) and the rose diagram (Figure 11). Fractures were situated in regions with mixtures of high and low intensity values. The FVD reported by Andrew et al.(2018) on Delineating Mineralisation Zones within the Keffi-Abuja area depicts a dominant NE-SW, NW-SE and E-W trends within the structural patterns and this shows similarities to the structural trends of NE-SW and NW-SE observed in this present study (Figures 9 and 10). The lineament map (Figure 10) shows similar trend with the drainage pattern (Figure 1) and this indicates that the drainage system could be structurally controlled.

Rose diagrams were plotted from visually extracted lineaments with the lengths of the rosette blades proportional to the square of the relative frequencies of the lineaments. The rose diagram (Figure 11) revealed that the dominant structural trend being in the NE – SW which corresponds to the major lineament trend while the NW-SE and N-S reflect the younger and deeper tectonic trends. However, the NE-SW trend reflects the older tectonic events, because the older events are more pronounced and tends to obliterate the younger events.

The Source Parameter Imaging revealed depth ranging from45.0 to 378.3 m (Figure 12). The deepest depth fall within the range value from 266.8 to 378.3 m (violet or pink) underlain by coarse porphyritic biotite hornblende granite, biotite hornblende, porphyroblastic gneiss and quartz. The shallow depth (blue) value ranges from 45.0 to 57.6 m (Figure 12) and is underlain by quartzite (Figure 2).

The depth to the first layer (D2) varies from 0.253 to 0.728 km (Figure 14) while second layer depth (D1) varies from 0.479 to 3.36 km (Figure 13) and this indicates that the average basement depth as deduced from power spectrum inversion is about 1.275 km (Table 1). The shallow magnetic sources are believed to be the resultant of basement rocks that were tectonically uplifted into the sedimentary overburden while the deeper basement depths may be attributed to lateral inversions in basement susceptibilities and intra basement structural features like faults, fractures and subductions (Ofoegbu and Onuoha, 1991; Kangoko et al,. 1997).

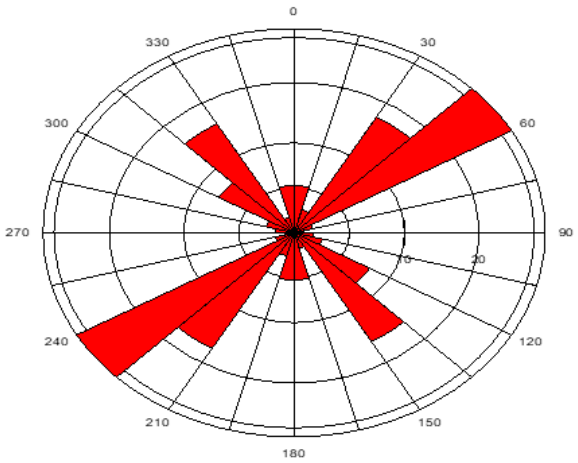

Figure 11: Rose diagram for Lineaments of Abuja sheet 186 and Gitata sheet 187

Science World Journal Vol. 16(No 3) 2021
www.scienceworldjournal.org
ISSN: 1597-6343 (Online), ISSN: 2756-391X (Print)
Published by Faculty of Science, Kaduna State University

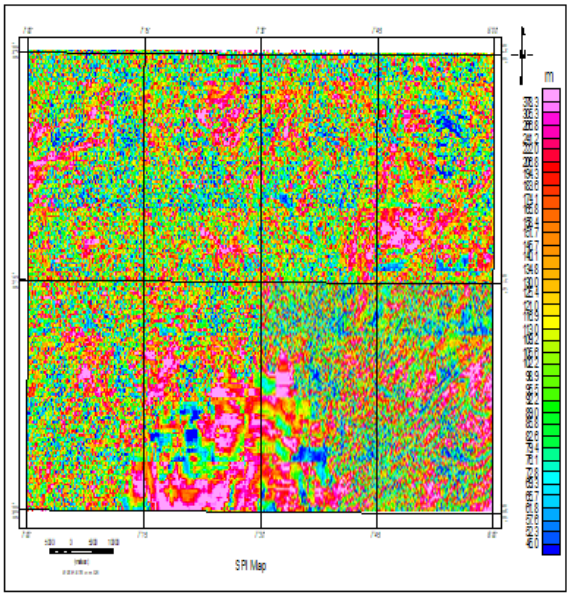

Figure 12: SPI Map of the Abuja sheet 186 and Gitata sheet 187

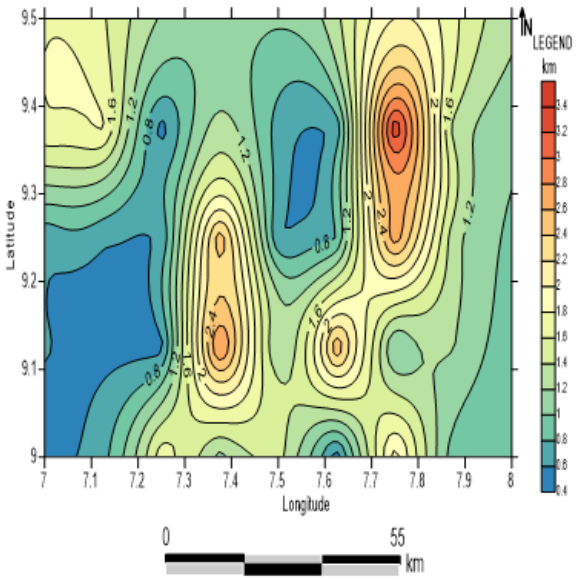

Figure 13: Deeper magnetic source depth (D_1) of Abuja sheet 186 and Gitata sheet 187

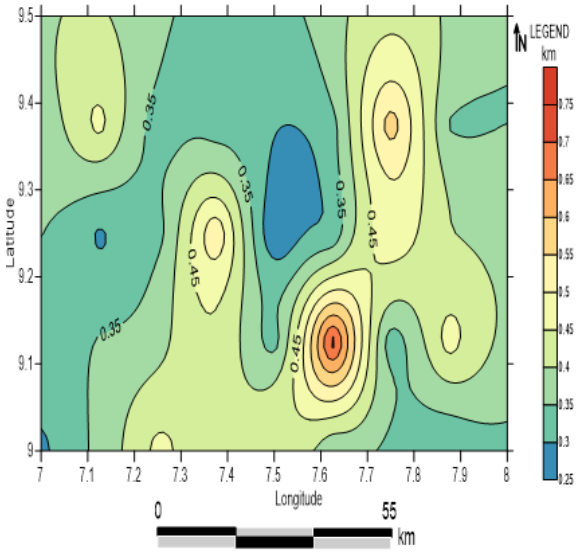

Figure 14: Shallow magnetic source depth (D_2) of Abuja sheet 186 and Gitata sheet 187

Conclusion

The total magnetic intensity values of the area ranges from 32919.5 to 33083.5nT. The high TMI value in the southern part of Gitata sheet depicts the presence of quartzite and granite-gneiss while the low TMI value indicates biotite-hornblende granite

Major trend of the lineament is NE-SW while minor trend is NW-SE. The orientation and length of the lineaments indicate that larger part of the rose diagram trends in the NE-SW and NNE-SSW directions with the NE-SW trends predominating

The deepest Spectral depth fall within the range value from 266.8 to 378.3 m (violet or pink) underlain by coarse porphyritic biotite hornblende granite, biotite hornblende, porphyroblastic gneiss and quartz. The shallow depth (blue) value ranges from 45.0 to 57.6 m (Figure 12) and is underlain by quartzite (Figure 2).

The depth to the first layer (D2) varies from 0.253 to 0.728 km while second layer depth (D1) varies from 0.479 to 3.36 km and this indicates that the average basement depth as deduced from power spectrum inversion is about 1.275 km.

REFERENCES

Adewumi, T., & Salako, K.O. (2017). Delineation of Mineral Potential Zone Using High ResolutionAeromagnetic Data Over part of Nasarawa State, North Central, Nigeria. Egyptian Journal of petroleum, 27(4), 75-765

Akanbi, E.S., & Fakoya, A.D. (2015). Regional Magnetic Field Trend and Depth to Magnetic Source Determination from Aeromagnetic Data of Maijuju Area, North Central, Nigeria. Physical Science Internaational Journal, 8(3): 1-13.

Ajakaiye, D.E., Hall, D.H., & Millar, T.W. (1985). Interpretation of aeromagnetic data across the central crystalline shield area of Nigeria. Geophys. J. R. astr. Soc. 83,503-517

Andrew, J., Alkali, A., Salako, K. A., & Udensi, E.E. (2018). Delineating Mineralisation Zones within the Keffi Abuja Area Using Aeromagnetic Data. Journal of Geography, Environment and Earth Science International, 15(3): 1-12,

Bello, R., Ofoha C.C., & Wehiuzo, N. (2017) . Geothermal Gradient, Curie Point Depth and Heat Flow Determination of Some Parts of Lower Benue Trough and Anambra Basin, Nigeria. Physical Science International Journal, 15(2): 1-11.

Ganiyu, S.A. (2012). Upward Continuation and Reduction to Pole Process on Aeromagnetic Data of Ibadan Area, South-Western Nigeria. Earth Science Research, 2 (1), 1927-0550

Kangoko, R., Ojo, S.B., & Umego, M.N. (1997). Estimation of Basement Depths in the Middle Cross River Basin by Spectral Analysis of the Aeromagnetic Field. Nig. Journal of Physics 9, 30-36.

Nabighian, M. N. (1972). The analytic signal of two dimensional magnetic bodies with polygonalcross-section.its properties and use for automated anomaly interpretation. Geophysics, 37(2), 507-517.

Obaje, N.G. (2009). Geology and Mineral Resources of Nigeria, 1-201.

Ofoegbu, C.O., & Onuoha, K.M. (1991). Analysis of Magnetic Data Over the Abakaliki Antichinorium of the Lower Benue Trough, Nigeria Marine and Petroleum Geology. 8, 174-183.

Parasnis, D.S. (1997). Applied Geophysics. Chapman and Hall, London, 21-27.

Reeves, C. (2005). Aeromagnetic Survey Principles, Practice and Interpretation. Geophysics, 1-12

Reynolds, R. L., Rosenbaum, J. G., Hudson, M. R., & Fishman, N. S. (1990). Rock magnetism, the distribution of magnetic minerals in the Earth's crust, and aeromagnetic anomalies: U. S. Geological Survey Bulletin 19(24), 24-45.

Thurston, S. (1997). Automatic conversion of magnetic data to depth, dip, and susceptibility contrast of peace River Arch area of northwestern Canada using the SPI (TM) method. Geophysics, 62 (3), 807–813